Energy-Dependent Excitation Cross Section Measurements of the Diagnostic Lines of Fe XVII

G. V. Brown, P. Beiersdorfer, H. Chen, and J. H. Scofield
University of California Lawrence Livermore National Laboratory, Livermore, California 94550, USA

K. R. Boyce, R. L. Kelley, C. A. Kilbourne, and F. S. Porter
NASA/Goddard Space Flight Center, Greenbelt, Maryland 20771, USA

M. F. Gu and S. M. Kahn
Department of Physics and Kavli Institute for Particle Astrophysics and Cosmology, Stanford University, Stanford, California 94305, USA

A. E. Szymkowiak
Department of Physics, Yale University, New Haven, Connecticut 06520, USA
(Received 19 January 2005; published 30 June 2006)

By implementing a large-area, gain-stabilized microcalorimeter array on an electron beam ion trap, the electron-impact excitation cross sections for the dominant x-ray lines in the Fe XVII spectrum have been measured as a function of electron energy establishing a benchmark for atomic calculations. The results show that the calculations consistently predict the cross section of the resonance line to be significantly larger than measured. The lower cross section accounts for several problems found when modeling solar and astrophysical Fe XVII spectra.

DOI: 10.1103/PhysRevLett.96.253201 PACS numbers: 34.80.Kw, 32.30.Rj, 32.80.Cy, 95.55.Ka

The emission from neonlike Fe^{16+} dominates the spectra of a plethora of nonterrestrial sources in the soft x-ray region between 10 and 17 Å. The high-resolution grating instruments on the Chandra and XMM-Newton x-ray observatories were designed to focus on this spectral region resulting in the highest quality spectra ever produced [1]. However, the diagnostic utility of the Fe XVII spectrum has been limited because modeling efforts have not been able to explain the intensity pattern of the emission from objects such as stellar coronae or galactic centers [2,3]. Problems had already existed in analyses of solar data [4], where it was found that spectra could only be adequately fitted by invoking resonance scattering. If present, this process mainly affects the dominant $1s^2 2s^2 2p^5_{1/2} 3d_{3/2}\,{}^1P_1 \rightarrow 1s^2 2s^2 2p^6\,{}^1S_0$ resonance transition, commonly labeled 3C [5]. Resonance scattering was, however, not a good explanation for many astrophysical sources [6]. For example, for star's other than the Sun where measured spectra are averaged over the emission from the star's entire observable surface, equal numbers of photons are scattered into and out of the observer's line of sight, eliminating the scattering effect. Resonance scattering also cannot explain many laboratory measurements of relative line ratios using electron beam ion traps and tokamaks [7–9], which are generally in agreement with those measured from nonterrestrial sources and have similar opacities.

A resolution of the problems associated with interpreting the Fe XVII spectra was suggested by Chen and Pradhan (CP) [10]. They performed a large-scale relativistic close-coupling (CC) calculation which predicts the line intensity of the $2p$-$3d$ transitions to have a strong energy dependence owing to the contribution from resonance excitation (RE). Their calculations were the first to provide excellent agreement with laboratory data from electron beam ion traps, which for Fe XVII existed only as relative cross sections, finding ratios of 2.95–3.27 for the intensity of 3C relative to the $1s^2 2s^2 2p^5_{3/2} 3d_{5/2}\,{}^3D_1 \rightarrow 1s^2 2s^2 2p^6\,{}^1S_0$ intercombination line 3D, compared to experimental ratios of 2.77–3.15 at three energies between 0.85 and 1.15 keV.

To provide a stringent test of theory, we have measured the absolute cross sections for the resonance lines 3C and 3D. The measurements show that, in the case of these lines, atomic theory generally predicts cross sections that are larger than measured. Moreover, we find that the lower measured cross sections remove discrepancies found between models and astrophysical observations.

Our measurements were carried out at the Lawrence Livermore National Laboratory's electron beam ion trap EBIT-I. EBIT-I was specifically designed for measuring electron excitation cross sections of x-ray transitions [11]; however, such measurements have been limited to transitions where uncertainty inherent in the unknown overlap between the source ions and the electron beam can be avoided by simultaneously measuring the photon emission from radiative recombination (RR) of beam electrons with source ions [11,12]. For Fe^{16+}, RR proceeds into the M-shell levels $3s$, $3p$, and $3d$ of Na-like Fe. The cross sections for RR into these levels is approximately 3 orders of magnitude smaller than the Fe XVII direct excitation cross sections, making the detection of the RR photons difficult and precluding measurements with available crystal spectrometers. Standard solid-state–type x-ray detectors used in previous measurements do not have the energy resolution to resolve such weak features among the emis-

sion from either neighboring charge states or indigenous impurity ions. For the present measurements, we used instead an x-ray microcalorimeter [13] to simultaneously record the x rays from direct excitation and RR of Fe XVII.

The x-ray spectrometer microcalorimeter (XRS) was developed at the NASA/Goddard Space Flight Center (GSFC) and consisted of a 6×6 array of 625×625 μm^2 pixels cooled to 60 mK, of which 30 were active during the present measurements. Each pixel has a long-time gain stability that extends beyond magnet cycles so no significant loss in energy resolution is seen when summing all pixels even after more than 1 d of continuous counting. The spectral response of the XRS has been photometrically calibrated between 300 eV and 10 keV [14] and was monitored on EBIT-I by recording the signal from an x-ray tube attached to the opposite viewport.

Using a ballistic gas injector, iron was continuously injected into EBIT-I as iron pentacarbonyl where it is ionized by the electron beam. The iron ions were then trapped radially by the potential of the electron beam and axially by the three drift tubes. The trap was emptied and refilled once every 3.5 s, minimizing the concentration of heavy impurities emanating from the electron gun to below one part in 10^4.

The XRS's $\sim$10 eV resolution across the 700–1500 eV band is sufficient to resolve the strongest Fe XVII lines from one another, as shown in Fig. 1. However, because Fe XVI inner-shell satellites fall within 10 eV of the lines 3C and 3D [7], we fielded a set of higher resolution crystal spectrometers to check for the presence of blends. Strong, easily observable x-ray emission from Fe XVI is present only during the injection phase of the EBIT-I cycle, when Fe XVI may dominate the charge balance for a short time as the iron charge distribution comes to equilibrium. These data are excluded from our analysis. Once the Fe charge

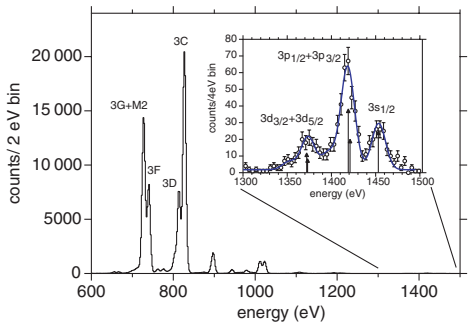

FIG. 1 (color online). Spectrum of Fe XVII measured by the NASA/GSFC 6×6 microcalorimeter array at an electron beam energy of 964 ± 5 eV. The inset shows a close-up view of the spectrum from only radiative recombination. The solid line represents the fit to five Gaussians, the three peaks from RR onto to Fe^{16+} and two peaks from background ions described in the text. The Fe^{16+} peaks, denoted by sticks with triangles, are labeled with the different fine structure components of Fe XVI. This spectrum is not corrected for filter transmittance or polarization effects.

distribution has reached an equilibrium, we estimate that less than 5% of the trapped ions are Fe^{15+}, and thus the influence of Fe XVI line emission on the Fe XVII lines is determined as a small correction as noted below.

The RR emission (Fig. 1) from the capture of a beam electron by Fe^{16+} ions can be described by

$$1s^2 2s^2 2p^6 + e^- \rightarrow 1s^2 2s^2 2p^6 3\ell_j + h\nu, \qquad (1)$$

where ℓ is s, p, or d, and j is $1/2$, $3/2$, or $5/2$. The photon energy $h\nu$ is equal to the sum of the binding energy of the recombined state and the energy of the captured electron. The energy difference between states of different orbital angular momentum ℓ is 40–50 eV and is resolved. However, the difference between states with the same ℓ is ≤ 2 eV and is not resolved. Two monoenergetic electron beam energy measurements were completed: one at 964 ± 5 eV and one at 910 ± 5 eV. The full width at half maximum energy spread of the electrons is $\sim$20 eV, as determined from fitting the RR peaks. These energies are consistent with the potential applied to accelerate the electrons. The electron density for these measurements is $10^{10} \leq n_e \leq 10^{11}$ cm^{-3}. There are $\sim 10^5$ total counts in the line 3C in Fig. 1, which is needed to accumulate more than 100 counts in the weakest RR peak.

The cross sections for direct excitation are determined by first normalizing the measured intensities of lines 3C and 3D to the measured intensity of the RR peaks, and then by normalizing the RR intensity to the theoretical RR cross section [11,12]. For the cross section of line 3C, this can be written as

$$\sigma_{3C}(E) = K(E)\sigma_j(E)\frac{I_{3C}}{I_j}, \qquad (2)$$

where $K(E)$ represents the combined correction for polarization, quantum efficiency, and filter transmission for both the RR photon and direct excitation photon emission, I_{3C} and I_j are the number of counts in the line 3C and RR peaks, respectively, and σ_j represents the known RR cross section for the level j. The cross sections for RR are determined from the theory given by Saloman *et al.* [15], which has been deemed accurate to within 5% or better provided the electron energy is high, as it is in our case. Polarization must be accounted for because of the monodirectional electron beam and the 90° viewing angle. The values of the polarization of the emitted RR radiation, $P = 1$ for $3s$ capture, 0.82 for $3p$, and 0.57 for $3d$, are provided by the same theory as the RR cross sections. The polarizations for direct excitation are calculated using the theory of Zhang *et al.* [16] and are $P = 0.40$ for both 3C and 3D.

The measured excitation cross sections at 964 eV for 3C based on normalizing to each of the three resolved RR peaks are given in Table I. The error associated with each measurement includes contributions from counting statistics, quantum efficiency, filter transmission, background, and polarization. For line 3C, in the case where the recombination onto the $3s$ level was used for normalization, those errors are 8%, 1%, 10%, 11%, and 5%, respectively. We

TABLE I. Results of the measurements at an electron-impact energy of 964 eV of the resonance line 3C normalized to each of the different RR states.

RR states used for normalization	σ_{RR} (cm^2) at 90°	σ_{3C} (cm^2)
$3s_{1/2}$	5.34×10^{-23}	$8.93 \pm 1.6 \times 10^{-20}$
$3p_{1/2} + 3p_{3/2}$	1.23×10^{-22}	$8.81 \pm 1.5 \times 10^{-20}$
$3d_{3/2} + 3d_{5/2}$	3.90×10^{-23}	$8.92 \pm 1.7 \times 10^{-20}$

note that no Fe^{17+} exists at this beam energy so enhancement of the Fe^{16+} lines resulting from recombination onto Fe^{17+} is not possible. Similarly, inner-shell ionization of Fe^{15+} cannot contribute.

If present, background ions with ionization energies near that of Fe^{16+}, such as C^{5+}, Ar^{8+}, Ar^{9+}, or Fe^{15+}, can contribute to the Fe XVII RR spectrum. We noticed a minor enhancement at photon energies of ~1355 and 1395 eV, which we tentatively identify as RR onto C^{5+} and Ar^{8+}. The contribution from these background ions adds less than 3% to the overall error. The agreement between the three cross sections derived by normalizing separately to the different RR peaks shows the internal consistency of the measurement. The cross sections of 3C for both 910 and 964 eV averaged over the RR peaks are given in Table II.

Before deriving the cross section for the intercombination line 3D, we took into account potential contributions from the Fe^{15+} inner-shell satellites, as indicated by the crystal spectrum, using the procedure discussed in Brown *et al.* [7]. After correcting for the Fe XVI contribution we obtained an intensity ratio of $I_{3C}/I_{3D} = 2.98 \pm 0.3$ and $I_{3C}/I_{3D} = 2.77 \pm 0.3$ for 964 and 910 eV, respectively. These are in excellent agreement with previous measurements and tabulated theoretical ratios given in [10].

Table II summarizes the measured cross sections and compares them with *R*-matrix calculations of Mohan *et al.* [17], the fully relativistic distorted-wave calculations of Zhang and Sampson [18], the close-coupling (*R*-matrix) calculations of CP [10], and the results of our own calculations using the relativistic distorted-wave (DW) Flexible Atomic Code (FAC). CP [10] include RE for levels up to $n \leq 4$. In the FAC we included RE of the type $n\ell n'\ell'$ where $n = 3$, 4, or 5 and $n' \leq 30$ as well as cascades from up to $n = 7$. We use the 30 eV Gaussian-averaged collision strengths of CP to derive the cross sections listed. The results from FAC are averaged over a 20 eV beam width.

Table II shows that our measured cross section of 3D agrees with the DW calculation of Zhang and Sampson and the RE-free *R*-matrix calculation. It is 30% lower than the result of the 89 level CC calculation by CP and 45% lower than the FAC calculation that includes RE and cascades. All four theories overestimate the cross section of 3C by ≥25%.

We also measured the excitation cross sections as a function of electron-impact energy utilizing an event-mode method in which the electron beam is swept linearly between two energies and each detected photon is tagged with the corresponding electron beam energy [19]. The results are plotted in Fig. 2. The *R*-matrix results and the FAC results with and without resonances are shown for comparison. At energies above 1150 eV for both 3C and 3D the energy dependence is well represented by either the *R*-matrix calculation of Mohan *et al.* or the FAC. However, in the case of 3C, both the *R* matrix and the FAC must be reduced by about 35% for 3C. For 3D, reducing the FAC result by 30% brings it into agreement. For FAC, cascade contributions enhance the cross section for 3C by less than 5% for all energies, and for 3D, less than 10%.

To compare the measured contribution from resonance excitation to the calculations, we have derived the resonance strength $S \equiv \int \sigma_{RE} dE$, where σ_{RE} represents the cross section for resonance excitation. We obtain for 3C $S_{3C}^{meas} = (1.6 \pm 1.1) \times 10^{-18}$ cm^2 eV and for 3D $S_{3D}^{meas} = (1.0 \pm 0.7) \times 10^{-18}$ cm^2 eV. Here the error is mainly due to the uncertainty in estimating the resonance-free background level. This compares to the resonance strength of CP of $S_{3C}^{CP} = 2.9 \times 10^{-18}$ cm^2 eV, $S_{3D}^{CP} = 1.9 \times 10^{-18}$ cm^2 eV, and those from FAC, $S_{3C}^{FAC} = 1.13 \times 10^{-18}$ cm^2 eV and $S_{3D}^{FAC} = 1.52 \times 10^{-18}$ cm^2 eV. In the

TABLE II. Comparison of measured and calculated cross sections for the Fe XVII resonance and intercombination x-ray lines.

Line	E_{e^-} (eV)	σ (cm^2)[a]	Theory[b]	Theory[c]	Theory[d]	Theory[e]
3C	964	$(8.88 \pm 0.93) \times 10^{-20}$	1.12×10^{-19}	1.19×10^{-19}	1.33×10^{-19}	1.30×10^{-19}
3C	910	$(8.49 \pm 1.6) \times 10^{-20}$	1.12×10^{-19}	1.21×10^{-19}	1.25×10^{-19}	1.26×10^{-19}
3D	964	$(2.98 \pm 0.33) \times 10^{-20}$	2.83×10^{-20}	3.14×10^{-20}	3.93×10^{-20}	4.37×10^{-20}
3D	910	$(3.10 \pm 0.64) \times 10^{-20}$	2.83×10^{-20}	3.19×10^{-20}	3.41×10^{-20}	4.17×10^{-20}

[a]This measurement.
[b]Mohan *et al.* [17]. These cross sections are calculated for 1088 eV.
[c]Zhang and Sampson [18].
[d]Chen and Pradhan [10]. These values are estimated from the collision strengths given in their Fig. 1(a) for 3C and Fig. 1(b) for 3D.
[e]Flexible Atomic Code.

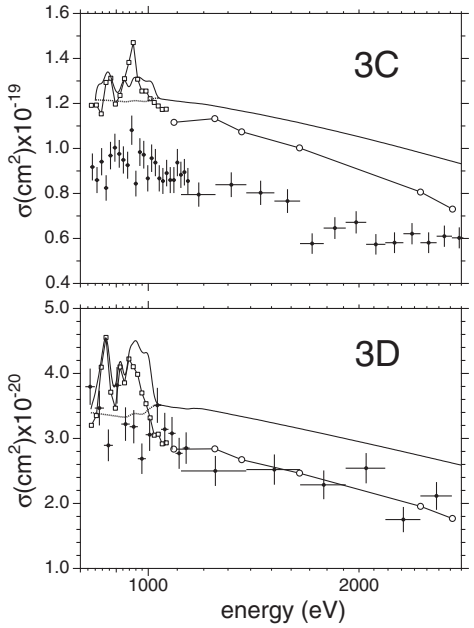

FIG. 2. Cross sections for the resonance line 3C (top panel) and intercombination line 3D (bottom panel) as a function of electron-impact energy given by solid circles. The error bars in the y direction are statistical and the error bars in the x direction denote the bin size. These curves are normalized to the single-energy measurement at $E_{e-} = 964$ eV. Each cross section is compared to the theories of Mohan *et al.* [17] (solid line with open circles), CP [10] (solid line with open squares), and the FAC calculations with (solid line) and without (dotted line) resonance excitation. The FAC is the only calculation that includes contributions from cascades.

case of our measurements and the calculations of CP, the lowest cross section value was used to calculate the baseline, resonance-free line strength. In the case of the FAC, the baseline is calculated directly and includes cascades. Comparing the resonance strength to the total line strength shows that, for both CP and FAC calculations, resonances contribute only a small amount. For 3C, the FAC resonances strength is 2% of the total, and for CP it is 5%. The measured enhancement is 4% ± 3%. Resonances contribute relatively more to 3D, for FAC, they add 9%, for CP 13%, and for the measurement, 9% ± 6%. The relatively small role played by resonances in the excitation of the upper level of 3C and 3D has been shown experimentally in high-Z neonlike ions and predicted theoretically for the case of Fe XVII [20], including the recent calculations of Loch *et al.* [21], and it implies that the discrepancy between theory and measurement lies in the calculation of the direct excitation cross section.

In summary, we have established a benchmark for testing calculations of cross sections of medium-Z neonlike ions. The results establish the use of microcalorimeters for measuring cross sections of ions with weak radiative electron capture rates inaccessible by earlier techniques. Our results demonstrate that, contrary to the implications by CP [10], the contributions from resonance excitation are not the source of discrepancy between theory and measurement. Our measurement has important implications for the analysis of astrophysical spectra and eliminates the need for invoking resonance scattering for explaining the reduced emission of 3C observed in many astrophysical sources relative to that expected from calculations. When no resonances or cascades are included, correct abundance measurements can be obtained by using the cross sections resulting from, for example, theoretical calculations for 3D but not for 3C. Our measurements thus provide a solution to the puzzling observations by Xu *et al.* [3] and Behar *et al.* [2] who in their study of NGC 4636 and Capella, respectively, found that consistent results were obtained only if they normalized their spectrum to 3D and not to 3C.

We acknowledge E. Magee, P. D'Antonio, and J. Gygax for their technical support. Work by the UC LLNL was performed under the auspices of the DOE under Contract No. W-7405-Eng-48 and supported by NASA APRA grants to LLNL, GSFC, and Stanford University.

[1] C. R. Canizares *et al.*, Astrophys. J. Lett. **539**, L41 (2000); A. C. Brinkman *et al.*, Astron. Astrophys. **365**, L324 (2001); S. M. Kahn *et al.*, Astron. Astrophys. **365**, L312 (2001).
[2] E. Behar *et al.*, Astrophys. J. **548**, 966 (2001).
[3] H. Xu *et al.*, Astrophys. J. **579**, 600 (2002).
[4] D. L. McKenzie *et al.*, Astrophys. J. **241**, 409 (1980); K. J. H. Phillips *et al.*, Astron. Astrophys. **324**, 381 (1997); K. Waljeski *et al.*, Astrophys. J. **429**, 909 (1994).
[5] J. H. Parkinson, Astron. Astrophys. **24**, 215 (1973).
[6] K. Wood and J. Raymond, Astrophys. J. **540**, 563 (2000).
[7] G. V. Brown *et al.*, Astrophys. J. Lett. **557**, L75 (2001).
[8] G. V. Brown *et al.*, Astrophys. J. **502**, 1015 (1998); P. Beiersdorfer *et al.*, Astrophys. J. **610**, 616 (2004); Phys. Rev. A **64**, 032705 (2001).
[9] P. Beiersdorfer *et al.*, Astrophys. J. Lett. **576**, L169 (2002).
[10] G. X. Chen and A. K. Pradhan, Phys. Rev. Lett. **89**, 013202 (2002).
[11] R. E. Marrs *et al.*, Phys. Rev. Lett. **60**, 1715 (1988).
[12] K. L. Wong *et al.*, Phys. Rev. A **51**, 1214 (1995).
[13] C. K. Stahle *et al.*, Phys. Today **52**, No. 8, 32 (1999); R. L. Kelley *et al.*, Proc. SPIE Int. Soc. Opt. Eng. **3765**, 114 (1999); F. S. Porter *et al.*, Rev. Sci. Instrum. **75**, 3772 (2004).
[14] M. D. Audley *et al.*, *Proceedings of a New Century of X-Ray Astronomy* (Astronomical Society of the Pacific, San Francisco, CA, 2001), p. 516.
[15] E. Saloman *et al.*, At. Data Nucl. Data Tables **38**, 1 (1988).
[16] H. L. Zhang *et al.*, Phys. Rev. A **41**, 198 (1990).
[17] M. Mohan *et al.*, Astrophys. J. **108**, 389 (1997).
[18] H. L. Zhang and D. H. Sampson, At. Data Nucl. Data Tables **43**, 1 (1989).
[19] D. Knapp, Z. Phys. D **S21**, S143 (1991); P. Beiersdorfer *et al.*, Rev. Sci. Instrum. **72**, 508 (2001).
[20] B. W. Smith *et al.*, Astrophys. J. **298**, 898 (1985); P. Beiersdorfer *et al.*, Phys. Rev. Lett. **65**, 1995 (1990); R. Doron and E. Behar, Astrophys. J. **574**, 518 (2002).
[21] S. D. Loch *et al.*, J. Phys. B **39**, 85 (2006).